(6) See, for example, P. E. Slade, Jr., Ed., "Polymer Molecular Weights", Part 1, Marcel Dekker, New York, 1975.
(7) B. Kronberg, D. F. R. Gilson, and D. Patterson, *J. Chem. Soc., Faraday Trans. 2*, **72**, 1673 (1976); D. E. Martire, G. A. Oweimreem, G. I. Ågren, S. G. Ryan, and H. T. Peterson, *J. Chem. Phys.*, **64**, 1456 (1976).
(8) G. Delmas, *J. Appl. Polymn. Sci.*, **12**, 839 (1968); H. G. Elias and H. Lys, *Macromol. Chem.*, **92**, 1 (1966).
(9) P. G. Assarson, P. S. Leung, and G. J. Stafford, *Polym. Prepr., Am. Chem. Soc., Div. Polym. Chem.*, **10**, 1241 (1969); J. L. Koenig and A. C. Angood, *J. Polym. Sci., Part A-2*, **8**, 1787 (1970); L. W. Kessler, W. D. O'Brien, and F. J. Dunn, *J. Phys. Chem.*, **74**, 4096 (1970); S. H. Maron and F. E. Filisko, *J. Macromol. Sci.-Phys.*, **6**, 79 (1972).

Electron Diffraction Investigation of a High-Temperature Form of Poly(vinylidene fluoride)

Andrew J. Lovinger* and H. D. Keith

Bell Laboratories, Murray Hill, New Jersey 07974. *Received February 12, 1979*

ABSTRACT: Thin films of poly(vinylidene fluoride), crystallized from the melt at temperatures above 160 °C, were examined by electron microscopy and diffraction. Immature spherulites of a high-melting form were found to be composed of collections of flat platelets with remarkably regular crystallographic growth facets. Electron diffraction patterns from these are not consistent with any of the commonly accepted unit cells for this polymer but are instead in agreement with a new unit cell that has recently been found in solution-grown samples and appears to be the correct one for γ-PVF_2. When tilted in the electron microscope, these melt-crystallized samples yielded diffraction patterns indicating that the molecular chains are not normal to the broad lamellar surfaces but are instead rotated about the b axis of the unit cell to an angle of 28.5° from the lamellar normal.

Poly(vinylidene fluoride) [PVF_2] is commonly obtained in two crystallographic modifications. The α form is the one predominantly observed during crystallization from the melt[1,2] and has been characterized by a large number of investigators.[3-13] Gal'perin et al.,[3,4] Natta and coworkers,[5] Doll and Lando,[6] and Hasegawa et al.[13] have analyzed its structure by X-ray diffraction; infrared spectroscopy has been employed by Cortili and Zerbi[8] and Enomoto et al.,[9] while Boerio and Koenig[10,11] have used Raman scattering. Farmer and co-workers[7] and Hasegawa et al.[12] have also applied potential energy calculations to the crystallographic study of α-PVF_2. Although minor differences in interpretation exist among these workers, the consensus has been that the α form consists of molecular chains adopting conformation II (essentially a slight variant of a $TGT\bar{G}$ conformation). On the basis of the latest crystallographic data,[13] the unit cell of α-PVF_2 is monoclinic (pseudo-orthorhombic), with a = 4.96 Å, b = 9.64 Å, c(chain axis) = 4.62 Å, and β = 90°, and contains two molecular chains.

The second major polymorph of PVF_2 is the β form, usually obtained by mechanical deformation of α spherulites. Its structure has been investigated by the above authors[3-5,7-9,12,13] and by others.[14-16] The molecular chains in β-PVF_2 adopt conformation I, which is either a fully planar zigzag[7,14] or a slight variant thereof, as suggested by Gal'perin and co-workers[3] and Hasegawa et al.[12,13] The latter authors found that to relieve the strain from adjacent fluorine atoms in an all-trans conformation, statistical deflections of CF_2 groups at an angle of 7° about the plane of the zigzag yield optimum experimental agreement both with X-ray intensities[13] and potential-energy calculations.[12] The unit cell of β-PVF_2 is orthorhombic and contains two molecules in a C-centered arrangement; its dimensions are a = 8.58° Å, b = 4.91 Å, and c(chain axis) = 2.56 Å.

In addition to these, two other polymorphs have been described in the literature. The γ form has been reported to grow from solution in dimethyl sulfoxide, dimethyl acetamide, and dimethyl formamide,[17,18] as well as from the melt at high pressures[19-21] and high temperatures.[1,2] On the basis of work by Hasegawa et al.,[13] its unit cell has for years been considered as only slightly different from that of β-PVF_2: the same number of molecular chains in the same conformation is thought to pack monoclinically with a = 8.66 Å, b = 4.93 Å, c(chain axis) = 2.58 Å, and β = 97°. However, an alternative γ-unit cell (discussed in detail later in this paper) has very recently been proposed by Weinhold et al.[22] The last known polymorph of PVF_2 has been reported[23,24] to be a polar version of the α form, obtained by rotation of alternate molecular chains under the influence of high electric fields.

As has been mentioned above, evidence for the crystal structures of the various polymorphs of PVF_2 has come almost exclusively from infrared and X-ray diffraction studies. Electron diffraction, whose ability to yield single crystal-like patterns from appropriate samples renders it particularly useful in structure determination, has only sporadically been applied to this polymer.[16,25-27] It is for this reason that we have undertaken a detailed electron microscopic study of melt-crystallized PVF_2. This paper consists of an analysis of electron diffraction data from certain crystalline regions whose structure could not be reconciled with any of the commonly accepted unit cells[13] for PVF_2; the morphological aspects of this investigation are described separately.[28]

Experimental Section

The PVF_2 samples studied were Kynar 821, obtained from Pennwalt Corp. Molecular weight averages, calibrated in terms of polystyrene fractions, were $\bar{M}_w$ = 541 000 and $\bar{M}_n$ = 337 000. Thin films of this polymer, suitable for electron microscopy, were deposited on freshly cleaved mica from dilute solution in dimethylformamide. The films were then melted and held at 200–220 °C for up to 30 min prior to recrystallization at the desired temperatures (ranging from 160 to 165 °C) in a Mettler FP5 microscope hot stage. After 24 h at 162 °C, gel permeation chromatography yielded $\bar{M}_w$ = 511 000 and $\bar{M}_n$ = 310 000, indicating that degradation had not occurred to any significant extent. Samples for electron microscopy were shadowed using

0024-9297/79/2212-0919$01.00/0

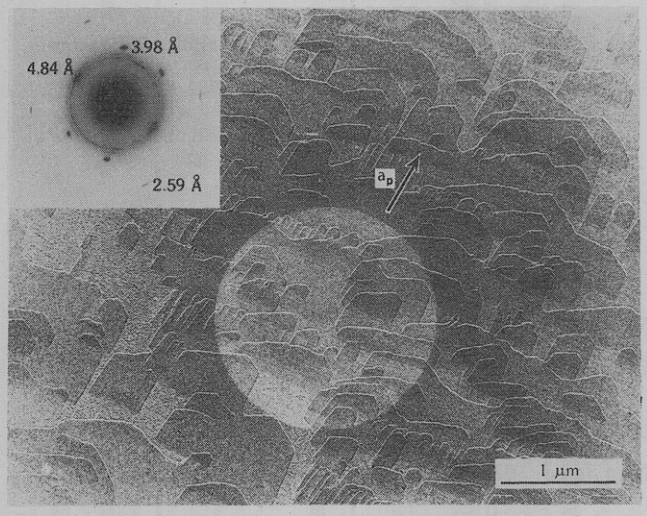

Figure 1. Electron micrograph of platelets of the high-temperature form of PVF_2 crystallized from the melt at 165 °C. The electron diffraction pattern shown in the inset is correctly oriented with respect to the field.

Pt–C in a vacuum evaporator and then coated with a thin layer of carbon. Calibrating substances (TlCl or Au) were also occasionally evaporated after carbon coating. Finally, the films were floated off the mica in distilled water and placed on copper grids for subsequent examination in a Philips EM 200 transmission electron microscope.

Results and Discussion

Two morphologically different crystalline species of PVF_2 were obtained in our samples. The lowest melting of these consisted of tightly banded spherulites whose electron diffraction patterns[28] identified them with the α form.[29] The higher-melting population appeared as immature spherulites (i.e., crystalline aggregates which had not yet reached cylindrical symmetry), consisting primarily of flat platelets. In very thin regions, monolayers 6–9-nm thick and a few μm in lateral dimensions were observed; most frequently, however, the samples were multilayered, as seen in Figure 1. The sharp faceting of these platelets is remarkable for a polymer of such high molecular weight crystallized from the melt and seems to imply fairly regular chain folding. These lamellae have been found[28] to grow simultaneously in two directions–along the arrow marked a_p in Figure 1 (as is seen later, this direction corresponds to the projection of a onto the lamellar surfaces) and normally to it. The latter direction appears to be dominant, insofar as it is the one that becomes radial in fully developed spherulites.[28]

The central portion of a selected area electron diffraction pattern obtained from the lighter region in Figure 1 is shown as an inset; a more complete pattern can be seen in Figure 2a. These patterns are dominated by sharp, single-crystal-like reflections and also exhibit the three amorphous rings (at about 4.80, 2.25, and 1.25 Å) characteristic of most carbon-chain polymers. In addition, two irregularly broken rings at spacings of ca. 4.89 and 4.52 Å are always present (see Figure 1). In some cases (particularly in patterns obtained from the smallest selected areas), these arcs appear to be centered on row lines defined by the dominant reflections. These arcs therefore suggest the presence of microcrystalline inclusions of a different phase interspersed within the main matrix. Further, these inclusions, though far from being well oriented, nevertheless appear to be aligned in a manner which reveals some tendency for registry with the lattice of the host. The interplanar spacings of these arcs are

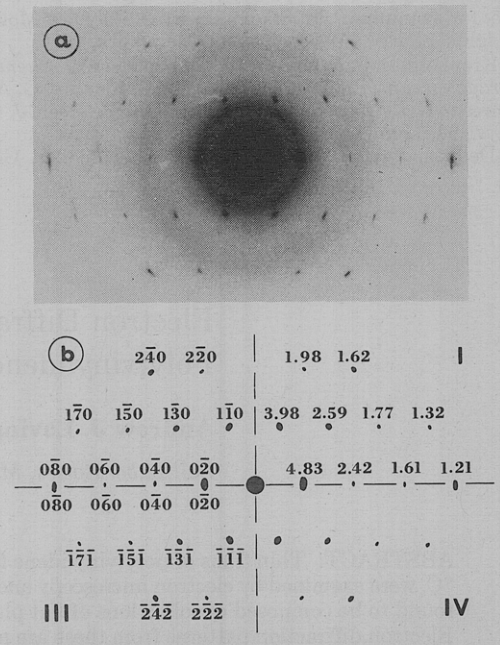

Figure 2. (a) A more extensive electron diffraction pattern from untilted PVF_2 platelets. (b) Schematic drawing of this pattern, showing observed d spacings in quadrant I and two possible sets of indices in quadrants II and III (see text).

slightly larger than those of the two strongest reflections of α-PVF_2, so that these inclusions may well consist of distorted microcrystallites of this phase.

Turning our attention now to the main features of the electron diffraction patterns of Figures 1 and 2a, we can at once see that these patterns are inconsistent with the generally accepted structures of all polymorphs of PVF_2.[13] Specifically, presence of the very strong reflection at 3.98 Å cannot be reconciled with the unit cells of the α, β, or γ phase as found by Hasegawa et al.[13] Having no reason to question the validity of these unit cells (whose structure was deduced on the basis of X-ray[13] and infrared data,[13,21,30] as well as of energetic calculations[12]), we originally thought that the diffraction patterns in Figures 1 and 2a originate from a new δ form of this polymer, whose possible structure we set out to determine.

Evaluation of unit cell dimensions required careful precautions to combat the effects of radiation damage which are particularly severe in this polymer. Not only is crystallinity in PVF_2 destroyed very rapidly during exposure to the electron beam, but the change is also preceded by large, anisotropic deformation of spherulites in the manner described by Grubb and Keller[31,32] for films of polyethylene. To minimize radiation effects, the sample was scanned not in the bright field but in the diffraction mode with very low beam intensities, small condenser apertures, and strong overfocus of the second condenser lens. Sample deformation was prevented by coating the polymer film on *both* sides with strong layers of evaporated carbon; the second layer was applied while the sample was on the grid in order to constrain it more effectively to its copper support. In this manner, the d spacings of the reflections seen in Figure 2a were found to be as presented in the first quadrant of Figure 2b.

Assuming that the molecular chains are perpendicular to the broad surfaces of the platelets in Figure 1 (as is commonly the case in polymer single crystals), the diffraction pattern of Figure 2a would correspond to the $hk0$ plane of the reciprocal lattice. Based on its clearly orthorhombic symmetry and on the systematic absence of reflections for which $h + k \neq 2n$, this pattern may then

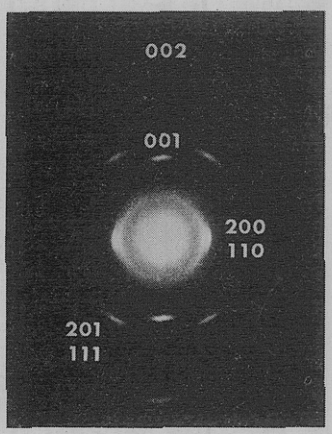

Figure 3. Electron diffraction pattern of mechanically drawn PVF_2 platelets, showing reflections attributable to the *c*-axis oriented β form.

be indexed as depicted in the second quadrant of Figure 2b, indicating apparent *a* and *b* unit cell axes equal to 4.35 and 9.66 Å, respectively. The length of the *c* axis could not be determined directly because our microscope was not equipped with a goniometer stage. Attempts to bring the molecular chains into the plane of the specimen by mechanical drawing yielded the electron diffraction pattern of Figure 3, from which a *c*-axis repeat of 2.56 Å, characteristic of a trans-planar conformation, is inferred. However, the spacings of all reflections in Figure 3 are characteristic of β-PVF_2, indicating that this diffraction pattern is the result of a transformation accompanying mechanical deformation, as is known to occur in this polymer.[13] The length of *c* was therefore estimated indirectly on the basis of two extra reflections at 1.65 and 1.29 Å which were observed occasionally in our single crystal-like patterns. The *d* spacings and relative dispositions of these reflections, coupled with the assumption that they are attributable to planes with $l = 1$, suggested *c*-axis repeat distances consistent with an all-trans conformation. An orthorhombic structure was deduced on this basis which represented, in essence, an affinely deformed β-unit cell. Calculated intensities of reflections were found to be in qualitative agreement with observed intensities; further, interatomic distances computed for trans-planar chains in such a cell did not show significant steric conflicts. On both of these counts, the presence of α-type chains (i.e., $TGTG\bar{}$) aligned normal to the (*ab*) basal plane of this cell was clearly impossible.

At this stage of our investigation, we learned that a new unit cell has been proposed for γ-PVF_2 by Weinhold, Litt, and Lando,[22] based upon X-ray fiber patterns of ultra-high molecular weight specimens crystallized from solution in dimethylacetamide and drawn at temperatures very close to the melting point. This unit cell is orthorhombic with dimensions a = 4.97 Å, *b* = 9.66 Å, and c(chain axis) = 9.18 Å. The 3.98-Å reflection found in our melt-crystallized samples is not incompatible with such a unit cell, as it is with the other unit cells of PVF_2.[13] If our specimens do indeed crystallize with this unit cell, then the diffraction pattern of Figure 2a could not represent the *hk*0 reciprocal lattice plane since the respective values for *a* in the two cases are significantly different. However, as the length of *b* in both cases is the same, the diffraction pattern of Figure 2a could potentially arise from the new γ-unit cell[22] if this were tilted about *b*, implying that the molecular chains are inclined to the broad surfaces of the lamellae.

To investigate this possibility, our specimens were examined in a Philips EM300 transmission electron microscope equipped with a goniometer stage.[33] Diffraction

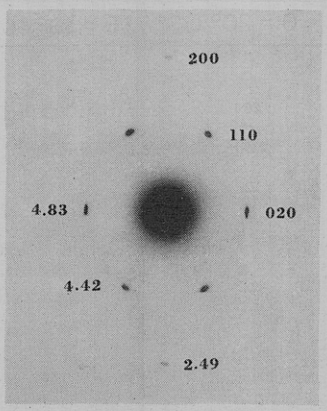

Figure 4. Electron diffraction pattern obtained from PVF_2 platelets tilted 30° clockwise about *b*.

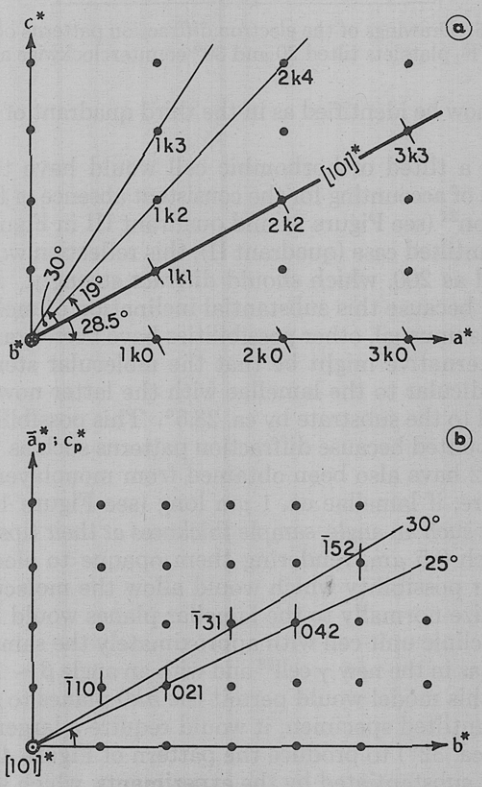

Figure 5. Schematic projections of the reciprocal lattice of the new γ-unit cell:[22] (*a*) along *b*; (*b*) along [101]*.

patterns were now obtained from areas less than 0.5 μm in diameter, as compared with 1–2 μm in the preceding experiments. Our samples were initially tilted at 5° intervals about *b*, spanning a range of ±45° from the untilted position. Clockwise and counterclockwise rotation by the same angle yielded *different* diffraction patterns, indicating that the symmetry of the unit cell is either lower than orthorhombic or that, if orthorhombic, the molecular chains are inclined with respect to the planes of the lamellae. The tilting sequence about *b* is dominated by a very intense pattern (see Figure 4) which is observed at a nominal tilt of 30° clockwise (the sense of tilt is defined by the reciprocal lattice projection along *b* shown in Figure 5a). The actual pattern depicted in Figure 4 was more extensive than shown, but the weaker reflections could not be reproduced photographically. This pattern could arise from the γ-unit cell of Weinhold et al.[22] if the *c* axes are inclined by 28.5° to the untilted specimen. In this case, Figure 4 would correspond to the *hk*0 section of the reciprocal lattice, while Figure 2a would then represent the *hkh* section; the indices of reflections seen in untilted films

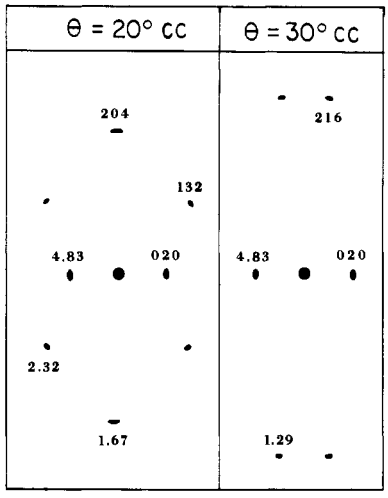

Figure 6. Drawings of the electron diffraction patterns obtained from PVF_2 platelets tilted 20 and 30° counterclockwise about *b*.

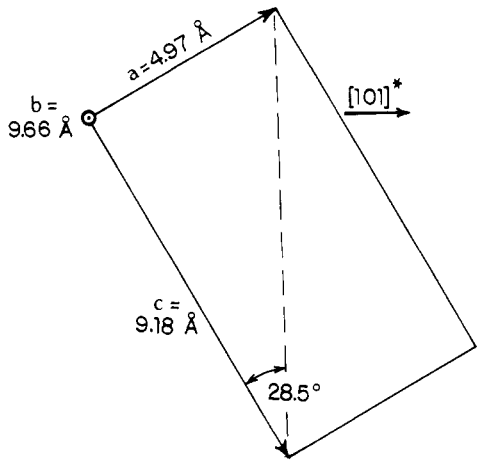

Figure 7. Projection of the unit cell of γ-PVF_2[22] along *b* in correct orientation within the lamellae. The broad lamellar surfaces are horizontal.

would now be identified as in the third quadrant of Figure 2b.

Such a tilted orthorhombic cell would have the advantage of accounting for the consistent absence of the 202 reflection[34] (see Figure 2a and quadrant III in Figure 2b); in the untilted case (quadrant II), this reflection would be indexed as 200, which should diffract strongly. Nevertheless, because this substantial inclination of molecular chains is unusual, other possibilities have been examined. One alternative might be that the molecular stems are perpendicular to the lamellae with the latter now being inclined to the substrate by ca. 28.5°. This possibility can be discounted because diffraction patterns such as that of Figure 2 have also been obtained from monolayers; furthermore, if lamellae ca. 1 μm long (see Figure 1) were tilted at such an angle, sample thickness at their tips would approach 0.5 μm, rendering them opaque to electrons. Another possibility which would allow the molecules to crystallize normally to the lamellar planes would invoke a monoclinic unit cell with approximately the same axial lengths as in the new γ cell[22] and with an angle $\beta \sim 118.5°$. While this model would permit the *hk*0 planes to reflect in the untilted specimen, it would require a larger angle of tilt (ca. 32°) to produce the pattern of Figure 4. This was not substantiated by the experiments, which showed maximal reflection intensities at 28–30°. A monoclinic cell would also be in conflict with the position of some reflections on the layer lines of X-ray diffraction patterns in oriented specimens.[22]

From all of the above, it appears that the molecular chains do indeed pack in the new γ-unit cell[22] and must therefore be inclined to the broad lamellar surfaces. The validity of this orthorhombic structure is further reinforced by diffraction data obtained by tilting in the opposite direction (i.e., counterclockwise in Figure 5a). Very weak patterns were observed at 20 and 30°, corresponding to the *hk*(2*h*) and *hk*(3*h*) reciprocal lattice sections, respectively (see Figure 5a); because these patterns were too weak to be reproduced photographically, they are drawn schematically in Figure 6. Both the positions of these reflections in the projected net and their interplanar spacings agree fully with the expected pattern from the orthorhombic cell[22] at these angles; however, the 102 reflection, which should appear at 19°, could not be detected in the very weak pattern of Figure 6.

One final point regarding the tilt sequence about *b* concerns the observation of very weak reflections at a quasi-110 disposition a few degrees before the major *hk*0 reflections come into view. The apparent *a*-axis repeat for these reflections is variable, ranging from 5.0 to 5.2 Å. This variability in spacing and the very low intensities lead us to ascribe them in part to a spike associated with 110 reciprocal lattice points and attributable to the thinness of the lamellar crystals.[35] As seen in Figure 5a, such a spike would be directed normally to the thin dimension of the platelets, i.e., along [10$\bar{1}$]. Since the lamellae were found by shadow casting to be ca. 60–90-Å thick (and therefore to contain only 7–11 unit cells between their surfaces), the average length of the reciprocal lattice spike on each side of the reflection is ~ 0.007 Å^{-1}. This would cause the intensity peak of the 110 reflections to extend out to an apparent *a*-axis spacing of 5.06 Å. The larger spacings occasionally observed could be due to contributions from the microcrystalline inclusions which, as mentioned previously, tend to reflect very closely to, and at larger spacings than, the (110) planes. Extra reflections are also observed occasionally in diffraction patterns from untilted specimens. While most such reflections were seen only rarely, an extra reflection was quite frequently visible at 1.29 Å; its *d* spacing and position within the reciprocal lattice grid would be consistent with 314 indices ($d = 1.33$ Å). Presence of this reflection in the *hkh* section would require a nominal tilt of $\sim 7°$ (which is actually smaller if the reciprocal lattice spike and the curvature of the Ewald sphere at this low spacing are taken into account) and is most probably attributable to lack of perfect flattness in electron microscopic specimens.

From all of the above, it is seen that the tilting sequence about *b* supports quite consistently an orthorhombic structure with molecular chains oblique to the lamellar normal, as drawn in Figure 7. This conclusion was further tested by a second tilt sequence, this time about an axis perpendicular to *b* and lying within the plane of the lamellae. This axis, which for the inclined orthorhombic case of Figure 7 is identified as [101]*, is essentially an arbitrary direction within the unit cell, contrary to the previous tilt axis (*b*) which represents a major crystallographic direction. The tilting process may be visualized with the aid of Figure 5b, which shows the reciprocal lattice projection down [101]*. Since *a* and *c* are now inclined with respect to this axis, they appear in projection (in this view, their projected lengths are equal and their directions opposite); *b* is seen in true measure.

Clockwise and counterclockwise tilting about [101]* yielded mirror images, as expected from Figure 5b. The most intense diffraction patterns were obtained between

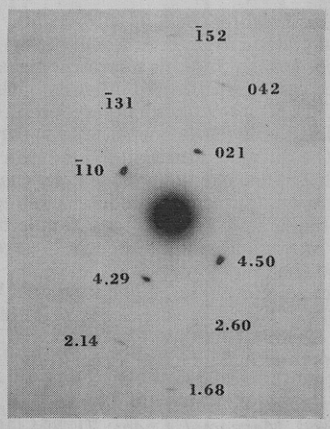

Figure 8. Electron diffraction pattern of PVF_2 platelets at a nominal tilt angle of 25° counterclockwise about [101]*.

25 and 30°; in this angular range, the electron beam is directed approximately parallel to $[\bar{2}12]$ for clockwise tilting (or to $[\bar{2}\bar{1}2]$ for counterclockwise). A typical diffraction pattern is seen in Figure 8, which also contains the observed interplanar spacings and assigned indices of reflections. With the sole exception of $\bar{1}10$ (to be discussed presently), excellent agreement is again obtained for all reflections as far as d spacings, geometrical dispositions within the pattern of Figure 8, and locations relative to the imaged section of the reciprocal lattice are concerned. Although the 021, $\bar{1}31$, 042, and $\bar{1}52$ reflections are not all coplanar in reciprocal space, lack of perfect flatness, together with the extent of reciprocal lattice spikes, will quite reasonably cause them to intersect reciprocal lattice planes between 25 and 30° (see Figure 5b); the low intensity (and occasional absence) of $\bar{1}31$ and $\bar{1}52$ reinforces this conclusion. However, the $\bar{1}10$ reflection is signficantly away from the imaged plane and should not be expected to appear, particularly at such high intensity, before a tilt of ~40° is attained (as a matter of fact, there are instances where $\bar{1}10$ is indeed absent or weak, but they do not constitute the rule). In addition, its observed interplanar spacing was found to be variable, ranging from 4.45 to 4.55 Å (i.e., 0.7–2.9% greater than d_{110}). Yet $\bar{1}10$ is the *only* reflection among the unit cells of all forms of PVF_2 that lies close to these spacings, and its indices are the *only* ones that would be compatible with the grid formed by the other reflections of Figure 8. Consequently, it appears that its usually strong intensity is to be ascribed to a combination of factors. The existence of a reciprocal lattice spike is undoubtedly one of them but could never alone produce such prominence. Some misorientation within the plane of the sample and, more importantly, localized deviations from true planarity (which are the overwhelming rule in these very thin films) are expected to play a major role in this regard. Finally, the increased and variable spacing may result in part from microcrystalline inclusions, as mentioned earlier, and from the foreshortening imparted by the reciprocal lattice spike.

General Discussion and Conclusions

Series of electron diffraction patterns from specimens tilted about two orthogonal axes lying in the plane of the film (i.e., b and [101]*) indicate that PVF_2 crystallizes from the melt at high temperatures with the same γ-unit cell as that found by Weinhold et al. for solution-grown films.[22] None of the evidence from our specimens is compatible with the original structure of the γ phase, as proposed by Hasegawa et al.[13] On the contrary, the validity of the new γ-unit cell[22] has now been demonstrated for both solution-[22] and melt-grown PVF_2 samples, using both X-ray diffraction on oriented specimens[22] and electron diffraction on essentially single crystals.

The two most striking features of these thin-film structures are their extraordinary crystallographic regularity and the substantial inclination of molecular stems to lamellar normals. From the angles measured in electron micrographs (e.g., Figure 1), the lamellae appear to be growing on their (020) and {110} faces. This very ordered morphology is reminiscent of that recently found by Bassett and Hodge[36] in polyethylene solidified from the melt at high temperatures and, in combination with their observations, shows that, at low supercooling, even polymers of high molecular weight can organize themselves in a very regular crystallographic fashion when crystallized from the melt.

Chain inclination of polymeric molecules within lamellae is, of course, well known for solution-grown single crystals from the work of Bassett and Keller[37] on polyethylene, Holland[38] on Nylon 66, and Yamashita[39] on poly(ethylene terephthalate). In a melt-crystallized polymer, this obliquity of the chains has been demonstrated by Bassett and Hodge[36] for polyethylene on the basis of a c-axis striation[40] observed in fracture surfaces; fold surfaces were thus found primarily to be {201}, with the molecular chains being inclined to the lamellar normal by 34.5°. In our case, electron diffraction has shown that the inclination is somewhat lower (28.5°); the lamellar surfaces are approximately parallel to $(20\bar{7})$. As in the polyethylene case, this chain inclination may be the result of crowding at fold surfaces.

Acknowledgment. We are greatly indebted to Dr. F. A. Khoury for his kindness in making his electron microscope available to us, for assistance in its operation, and for helpful discussions. We would also like to thank Drs. J. B. Lando and S. Weinhold for providing us with a copy of their paper prior to publication and Dr. G. T. Davis for helpful discussions and suggestions.

References and Notes

(1) W. M. Prest and D. J. Luca, *J. Appl. Phys.*, **46**, 4136 (1975).
(2) W. M. Prest and D. J. Luca, *J. Appl. Phys.*, **49**, 5042 (1978).
(3) Ye. L. Gal'perin, Yu. V. Strogalin, and M. P. Mlenik, *Vysokomol. Soedin.*, **7**, 933 (1965).
(4) Ye. L. Gal'perin and B. P. Kosmynin, *Vysokomol. Soedin.*, **11**, 1432 (1969).
(5) G. Natta, G. Allegra, I. W. Bassi, D. Sianesi, D. Kaporiccio, and E. Torti, *J. Polym. Sci., Part A*, **3**, 4263 (1965).
(6) W. W. Doll and J. B. Lando, *J. Macromol. Sci., Phys.*, **4**, 309 (1970).
(7) B. L. Farmer, A. J. Hopfinger, and J. B. Lando, *J. Appl. Phys.*, **43**, 4293 (1972).
(8) G. Cortili and G. Zerbi, *Spectrochim. Acta, Part A*, **23**, 285 (1967).
(9) S. Enomoto, Y. Kawai, and M. Sugita, *J. Polym. Sci., Part A-2*, **6**, 861 (1968).
(10) F. J. Boerio and J. L. Koenig, *J. Polym. Sci., Part A-2*, **7**, 1489 (1968).
(11) F. J. Boerio and J. L. Koenig, *J. Polym. Sci., Part A-2*, **9**, 1517 (1971).
(12) R. Hasegawa, M. Kobayashi, and H. Tadokoro, *Polym. J.*, **3**, 591 (1972).
(13) R. Hasegawa, Y. Takahashi, and H. Tadokoro, *Polym. J.*, **3**, 600 (1972).
(14) J. B. Lando, H. G. Olf, and A. Peterlin, *J. Polym. Sci., Part A-1*, **4**, 941 (1966).
(15) J. B. Lando and W. W. Doll, *J. Macromol. Sci., Phys.*, **2**, 205 (1968).
(16) K. Okuda, T. Yoshida, M. Sugita, and M. Asahina, *J. Polym. Sci., Part B*, **5**, 465 (1967).
(17) G. Cortili and G. Zerbi, *Spectrochim. Acta, Part A*, **23**, 2216 (1967).
(18) Ye. L. Gal'perin, B. P. Kosmynin, and R. A. Bychkov, *Vysokomol. Soedin., Ser. B*, **12**, 555 (1970).
(19) W. W. Doll and J. B. Lando, *J. Macromol. Sci., Phys.*, **2**, 219 (1968).

(20) W. W. Doll and J. B. Lando, *J. Macromol. Sci., Phys.*, 4, 889 (1970).
(21) R. Hasegawa, Y. Tanabe, M. Kobayashi, H. Tadokoro, A. Sawaoka, and N. Kawai, *J. Polym. Sci., Part A-2*, 8, 1073 (1970).
(22) S. Weinhold, M. H. Litt, and J. B. Lando, *J. Polym. Sci., Polym. Lett. Ed.*, in press.
(23) G. T. Davis, J. E. McKinney, M. G. Broadhurst, and S. C. Roth, *J. Appl. Phys.*, 49, 4998 (1978).
(24) D. Naegele, D. Y. Yoon, and M. G. Broadhurst, *Macromolecules*, 1297 (1978).
(25) K. Sakaoku and A. Peterlin, *J. Macromol. Sci., Phys.* 1, 401 (1967).
(26) R. L. Miller and J. Raisoni, *J. Polym. Sci., Polym. Phys. Ed.*, 14, 2325 (1976).
(27) Ye. L. Gal'perin, V. F. Myndrul, and V. K. Smyrnov, *Vysokomol. Soedin., Ser. A*, 12, 1949 (1970).
(28) A. J. Lovinger, *J. Polym. Sci., Polym. Phys. Ed.*, in press.
(29) A. J. Lovinger and T. T. Wang, *Polymer*, 20, 725 (1979).
(30) M. Kobayashi, K. Tashiro, and H. Tadokoro, *Macromolecules*, 8, 158 (1975).
(31) D. T. Grubb and A. Keller, *J. Mater. Sci*, 7, 822 (1972).
(32) D. T. Grubb, *J. Mater. Sci.*, 9, 1715 (1974).
(33) We are most grateful to Dr. F. A. Khoury of the National Bureau of Standards for making this microscope available to us.
(34) In this tilted case, the diffracted intensity of the 202 reflections can be thought of as arising from every second of four segments corresponding to the four monomeric units per repeat distance. Although the diffracted intensity from each of these will be slightly different depending upon the exact chain conformation, for all intents and purposes these intensities can be considered essentially the same. Therefore, the 202 reflection should suffer destructive interference, while 404 ought to be reasonably strong, as is indeed the case.
(35) P. B. Hirsch, A. Howie, R. B. Nicholson, D. W. Pashley, and M. J. Whelan, "Electron Microscopy of Thin Crystals", Butterworths, London 1965.
(36) D. C. Bassett and A. M. Hodge, *Proc. R. Soc. London, Ser. A*, 359, 121 (1978).
(37) D. C. Bassett and A. Keller, *Philos. Mag.*, 6, 345 (1961).
(38) V. F. Holland, *Makromol. Chem.*, 71, 204 (1964).
(39) Y. Yamashita, *J.Polym. Sci., Part A*, 3, 81 (1965).
(40) D. C. Bassett, *Polymer*, 17, 460 (1976).

High-Resolution Carbon-13 Nuclear Magnetic Resonance of Solid Poly(oxymethylene)

W. S. Veeman,* E. M. Menger, W. Ritchey,‡ and E. de Boer

Department of Physical Chemistry, University of Nijmegen, Toernooiveld, 6525 ED Nijmegen, The Netherlands. *Received March 13, 1979*

ABSTRACT: ^{13}C spectra and relaxation times were determined for poly(oxymethylene) at 45 MHz with proton-decoupled magic-angle-spinning NMR with and without cross-polarization. The results indicate the coexistence of two phases: a crystalline phase with short $T_{1\rho}$ and long T_1 and an amorphous phase with a longer $T_{1\rho}$ and a shorter T_1. These results are consistent with crystallinity measurements on the same samples by X-ray diffraction. The crystalline $T_{1\rho}$, which is not thought to be a pure spin–lattice relaxation parameter but is also determined by spin–spin interaction, depends on the spinning frequency. At high spinning frequency ($>\sim 5$ kHz), the line width (at magic-angle-spinning conditions) increases with an increase in the spinning frequency.

By combining heteronuclear decoupling and cross-polarization techniques[1] with magic-angle spinning, Schaefer and Stejskal[2] have clearly demonstrated that high-resolution NMR of solids is possible. Since then they obtained high-resolution ^{13}C spectra of a number of polymers and showed that one can measure ^{13}C spin–relaxation parameters for every ^{13}C spin which gives a resolved NMR line.[3,4] These relaxation parameters include the spin–lattice relaxation time T_1, the rotating frame spin–lattice relaxation time $T_{1\rho}$, and the ^1H–^{13}C cross-polarization time T_{CH}.

This study concerns a simple polymer, poly(oxymethylene), which under magic-angle-spinning conditions gives one, rather narrow, line. $T_{1\rho}$ measurements, however, reveal clearly that this line consists of two components with very different relaxation behavior. These components are attributed to crystalline and amorphous regions in the material. While this information can also be obtained from a nonspinning sample in this particular simple case, for polymers with chemically different carbons this is not possible due to overlapping powder line shapes. Thus for more complicated polymers, $T_{1\rho}$ (or any other relaxation parameter, of course) measurements under magic-angle-spinning conditions can be performed in order to determine the crystallinity of the polymers.

The ^{13}C $T_{1\rho}$ is measured via the decay of the rotating frame ^{13}C magnetization in a resonant radiofrequency field H_1. Although the notation $T_{1\rho}$ suggests spin–lattice relaxation, spin–spin processes can contribute significantly to this $T_{1\rho}$, especially when H_1 is not at least an order of magnitude larger than the local field.[4,5] While it is interesting to determine the relative contributions of spin–spin and spin–lattice relaxation to $T_{1\rho}$, we do not make such an attempt here.

Experimental Section

The NMR spectrometer is home built around a wide-bore (110 mm) 4.2 T superconducting magnet (Oxford Instruments). The ^{13}C H_1 field used has a rotating component amplitude corresponding to a frequency of 25 kHz. The spinner for magic-angle spinning is of a new design;[6] it has a cylindrical shape (diameter 10 mm) and is supported by two air bearings. Spinning frequencies between 500 and 5600 Hz can be maintained with excellent long-term stability (i.e., routine weekend operation). For the study reported here, the spinner was machined from Delrin, but for other polymers hollow KEL-F spinners have been used.

The $T_{1\rho}$ measurements were completely automatized such that the hold time τ (Figure 1) was varied after each FID. In most cases, 16 τ values were selected, and the corresponding 16 FID's were accumulated separately. This has the advantage that any slow drift of any experimental parameter does not affect the $T_{1\rho}$ plots. With regard to the $T_{1\rho}$ plots, it should be noted that the first point is taken after 100 μs, and under these conditions no $T_{1\rho}$ dispersion is found as reported by Schaefer et al.[3] except for the biexponential decay reported below.

^{13}C spectra and ^{13}C $T_{1\rho}$'s are determined both with and without cross-polarization. In the latter case, ^{13}C magnetization was prepared by a 90° pulse. The two pulse sequences for the $T_{1\rho}$ measurements are shown in Figure 1.

‡ On leave from Case Western Reserve University, Cleveland, Ohio.

0024-9297/79/2212-0924$01.00/0